Vol 17 No 11, November 2008
1674-1056/2008/17(11)/4184-09

Chinese Physics B

© 2008 Chin. Phys. Soc.
and IOP Publishing Ltd

Retrieval algorithm of quantitative analysis of passive Fourier transform infrared (FTRD) remote sensing measurements of chemical gas cloud from measuring the transmissivity by passive remote Fourier transform infrared*

Liu Zhi-Ming (刘志明)†, Liu Wen-Qing(刘文清), Gao Ming-Guang(高闽光), Tong Jing-Jing (童晶晶), Zhang Tian-Shu (张天舒), Xu Liang(徐 亮), and Wei Xiu-Li(魏秀丽)

Key Laboratory of Environmental Optics & Technology, Chinese Academy of Sciences, Hefei 230031*, China*
Anhui Institute of Optics and Fine Mechanics, Chinese Academy of Sciences, Hefei 230031*, China*

(Received 8 April 2008; revised manuscript received 16 May 2008)

Passive Fourier transform infrared (FTIR) remote sensing measurement of chemical gas cloud is a vital technology. It takes an important part in many fields for the detection of released gases. The principle of concentration measurement is based on the Beer–Lambert law. Unlike the active measurement, for the passive remote sensing, in most cases, the difference between the temperature of the gas cloud and the brightness temperature of the background is usually a few kelvins. The gas cloud emission is almost equal to the background emission, thereby the emission of the gas cloud cannot be ignored. The concentration retrieval algorithm is quite different from the active measurement. In this paper, the concentration retrieval algorithm for the passive FTIR remote measurement of gas cloud is presented in detail, which involves radiative transfer model, radiometric calibration, absorption coefficient calculation, *et al.* The background spectrum has a broad feature, which is a slowly varying function of frequency. In this paper, the background spectrum is fitted with a polynomial by using the Levenberg–Marquardt method which is a kind of nonlinear least squares fitting algorithm. No background spectra are required. Thus, this method allows mobile, real-time and fast measurements of gas clouds.

Keywords: passive remote measurement, Fourier transform infrared (FTIR), gas cloud sensing, concentration retrieval
PACC: 3320E, 8670L, 0765G, 3300

1. Introduction

The technology of Passive FTIR remote measurement has several advantages:[1] fast measurement of multi-component, passive remote sensing at a long distance, no requirement for artificial IR sources, and measurement on moving platforms. This technology is widely used to detect the released gases over a distance. The gases released from a chemical factory in the case of chemical accidents may be highly toxic. In order to protect workers at site and residents nearby, the identification and the quantification of the released gases are required. There are also military requirements for the remote detection and warning of chemical and biological warfare vapours and aerosols.[2] In most cases, buildings, trees and sky are taken as background.[3] The difference between the temperature of the gas cloud and the brightness temperature of the background is usually a few kelvins. The gas cloud emission is almost equal to the background emission. The acquirement of the emission of the gas cloud and the background becomes the primary task, which determines the accuracy of the results.

In this paper, the concentration retrieval algorithm for the passive FTIR remote measurement of gas cloud is presented in detail. A simulated experiment for sulfur hexafluoride (SF_6) is performed in laboratory. The calculated spectrum accords well with the measured spectrum. The concentration retrieval algorithm is proved by the results.

*Project supported by the National Natural Science Foundation of China (Grant No 083H311501) and the National High Technology Research and Development Program of China (Grant No 073H3f1514).
†E-mail: zhimingliu@aiofm.ac.cn or liuzhiming168@163.com

2. Theory

2.1. Planck's radiation law

In terms of Planck's radiation law, the radiation of a blackbody at temperature T is given by[4]

$$B(\nu,T)=\frac{C_1\nu^3}{\exp(C_2\nu/T)-1}, \tag{1}$$

where ν is the wavenumber (cm^{-1}), T is the absolute temperature (K), $C_1=1.191062\times10^{-12}\mathrm{W}\cdot\mathrm{cm}^2/\mathrm{sr}$ is the first radiation constant, and $C_2=1.438786\,\mathrm{K}\cdot\mathrm{cm}$ is the second radiation constant. If the radiation spectrum of an object is known, with the inverse function of Planck's radiation law, the spectrum of brightness temperature is computed from

$$T(\nu)=\frac{C_2\nu}{In\left(\dfrac{C_1\nu^3}{B(\nu)}+1\right)}. \tag{2}$$

2.2. Radiative transfer model

In many cases, the three-layer model can be used as shown in Fig.1, in which the atmosphere is divided into three plane-parallel homogeneous layers along the optical path.[5] From Fig.1, it is shown that the radiance L_1 entering into the FTIR spectrometer includes the radiance of the cloud (layer 2), the radiance of the atmosphere (layer 1) between the cloud and the FTIR spectrometer and the radiance of the background (layer 3) after absorption by the cloud and the atmosphere.[6] It can be expressed as

$$\begin{aligned}L_1(\nu)\;=\;&\varepsilon_1(\nu)B_1(\nu,T_1)+\tau_1(\nu)[\varepsilon_2(\nu)B_2(\nu,T_2)\\&+\tau_2(\nu)L_3(\nu)],\end{aligned} \tag{3}$$

where $\varepsilon_i(\nu)$ is the emissivity of layer i, $B_i(\nu,T_i)$ is the radiance of a blackbody at a temperature of layer i, T_i, and $L_3(\nu)$ is the radiance of background.

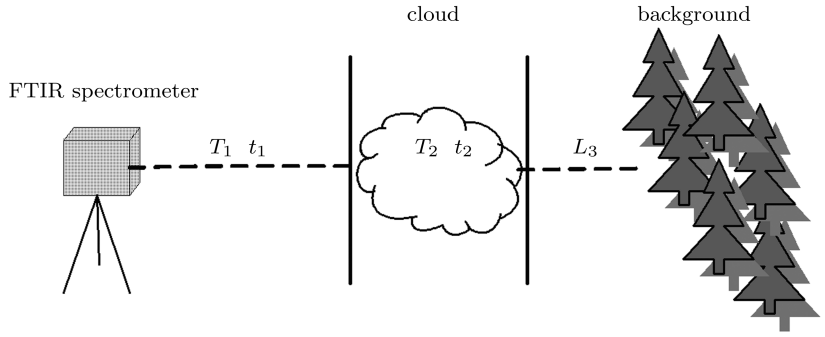


Fig.1. Schematic of the three-layer model.

The radiance will be absorbed, transmitted and scattered (or reflected) when transmitting in the atmosphere, but the tall power is conservative,[7,8] i.e.

$$\alpha+\tau+\rho=1, \tag{4}$$

where α is absorptivity, τ is transmissivity, and ρ is reflectivity. All of them are frequency dependent. In practice, the effects of reflectivity are often negligible ($\rho\approx0$), and so expression (4) is simplified into

$$\alpha+\tau=1. \tag{5}$$

Kirchoff's law states that

$$\alpha=\varepsilon, \tag{6}$$

where ε is emissivity. Expression (5) is changed into

$$\varepsilon+\tau=1. \tag{7}$$

Substituting expression (7) into expression (3) yields

$$\begin{aligned}L_1(\nu)\;=\;&(1-\tau_1(\nu))B_1(\nu,T_1)+\tau_1(\nu)[(1-\tau_2(\nu))\\&\times B_2(\nu,T_2)+\tau_2(\nu)L_3(\nu)].\end{aligned} \tag{8}$$

In the passive remote measuring of chemical gas, generally, one has to work in a spectral region, in which water and CO_2 are not absorbed strongly. This region is called atmosphere window, in which the transmissivity of the atmosphere is high ($\tau_1(\nu)\approx1$). In practice, it is assumed that the temperatures of the chemical gas cloud and the ambient atmosphere are equal, thereby $B_1(\nu,T)=B_2(\nu,T)=B(\nu,T)$, where T is the temperature of ambient atmosphere. Thus, expression (8) can be simplified into

$$L_1(\nu)=(1-\tau_2(\nu))B(\nu,T)+\tau_2(\nu)L_3(\nu). \tag{9}$$

According to expression (9), the transmissivity ($\tau_2(\nu)$)

of the cloud can be calculated as

$$\tau_2(\nu) = \frac{L_1(\nu) - B(\nu, T)}{L_3(\nu) - B(\nu, T)}. \quad (10)$$

3. Experiment

Since the purpose of this paper is to introduce the algorithm of passive FTIR remote sensing measurements of chemical gas cloud, a simulated experiment was performed in laboratory in Hefei, Anhei Province, China on 6th March 2008. The temperature of the ambient atmosphere was measured by using a thermometer. It was 8°C. In the laboratory, sulfur hexafluoride (SF_6) was released as the target gas. Because sulfur hexafluoride (SF_6) is one of the most popular insulating gases (next to air). It has a number of nice properties: not flammable, non-toxic, moderately inexpensive, and especially very strong adsorption at 950 cm^{-1}. The spectrum was measured by using an MR154 FTIR spectrometer with a narrow angle input telescope (SMY02) and a blackbody calibration source whose temperature error is estimated to be ±0.1°C. The temperature controlled was 24.1°C. Sulfur hexafluoride (SF_6) was released from a vessel between the spectrometer and the blackbody source, which served as the background in this experiment. Measurements were performed approximately 5 m far from the vessel. The schematic of the measurement is shown in Fig.2. The spectrum was acquired with a liquid-nitrogen-cooled, narrow band, mercury-cadmium telluride (MCT) detector at a 4 cm^{-1} spectral revolution. Because sulfur hexafluoride (SF_6) has a broad absorption band at 950 cm^{-1}, the 4cm^{-1} spectral revolution is sufficient for the measurement.

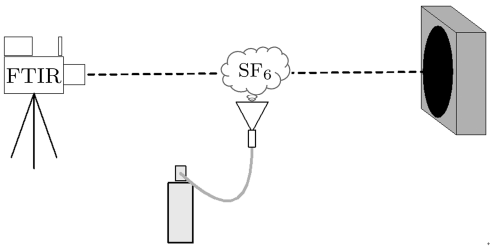


Fig.2. Schematic diagram of the experimental setup.

Figure 3 shows the measured result (un-calibrated spectrum) with sulfur hexafluoride (SF_6). In order to calculate the transmissivity of the gas cloud from expression (10), the raw spectrum (un-calibrated spectrum) should be converted into a radiance spectrum (calibrated spectrum) through radiometric calibration.

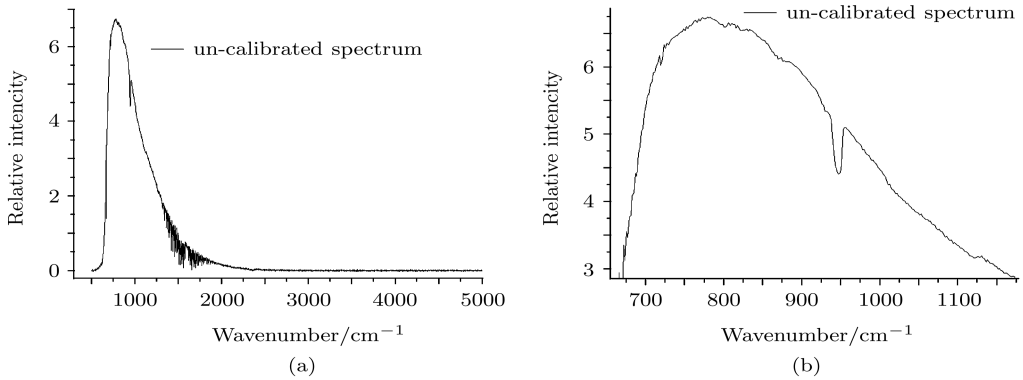


Fig.3. Un-calibrated spectrum of the measurement with sulfur hexafluoride (SF_6).

4. Data analysis and processing

4.1. Radiometric calibration

The ideal radiometer is a linear instrument, i.e. the measured signal for each pixel and each spectral channel is proportional to the radiant spectral power at detector[9,10] as illustrated in Fig.4. The slope of the line represents the instrument response, and the line does not cross the abscissa at $x = 0$ but rather at some value corresponding to the thermal emission of the spectrometer itself.[8]

The calibration formula can be expressed as

$$L^{\text{Measured}}(\nu) = K(\nu)(B^{\text{Source}}(\nu, T) + M^{\text{stray}}(\nu)), \quad (11)$$

where $L^{\text{Measured}}(\nu)$ is the measured complex spectrum, $K(\nu)$ is the complex instrument response function ($cm^2 \cdot sr \cdot cm^{-1}/W$), $B^{\text{Source}}(\nu, T)$ is the theoretical spectral radiance ($W/cm^2 \cdot sr \cdot cm^{-1}$) of the black-

body; and $M^{\text{stray}}(\nu)$ is the spectral power of the stray

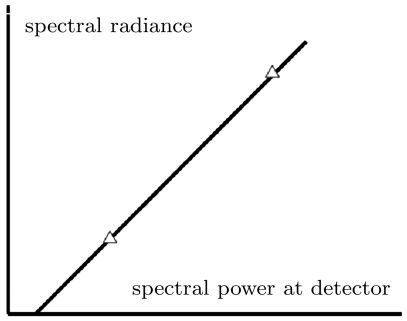


Fig.4. Linear relationship between spectral radiance and power at the detector.

radiance($\text{W/cm}^2 \cdot \text{sr} \cdot \text{cm}^{-1}$). Two measurements are required to determine the values of $K(\nu)$ and $M^{\text{stray}}(\nu)$, i.e.

$$L_{\text{H}}^{\text{Measured}}(\nu) = K(\nu)(B_{\text{H}}^{\text{Measured}}(\nu, T_{\text{H}}) + M^{\text{stray}}(\nu)) \quad (12)$$

and

$$L_{\text{C}}^{\text{Measured}}(\nu) = K(\nu)(B_{\text{C}}^{\text{Measured}}(\nu, T_{\text{C}}) + M^{\text{stray}}(\nu)), \quad (13)$$

where $L_{\text{H}}^{\text{Measured}}(\nu)$ and $L_{\text{C}}^{\text{Measured}}(\nu)$ are the measured spectra of the blackbody with hot and cold temperatures respectively. $B_{\text{H}}^{\text{Measured}}(\nu, T_{\text{H}})$ and $B_{\text{C}}^{\text{Measured}}(\nu, T_{\text{C}})$ are calculated from expression (1), then

$$K(\nu) = \frac{L_{\text{H}}^{\text{Measured}}(\nu) - L_{\text{C}}^{\text{Measured}}(\nu)}{B_{\text{H}}^{\text{Measured}}(\nu, T_{\text{H}}) - B_{\text{C}}^{\text{Measured}}(\nu, T_{\text{C}})} \quad (14)$$

and

$$M^{\text{stray}}(\nu) = \frac{B_{\text{H}}^{\text{Measured}}(\nu, T_{\text{H}}) L_{\text{C}}^{\text{Measured}}(\nu) - B_{\text{C}}^{\text{Measured}}(\nu, T_{\text{C}}) L_{\text{H}}^{\text{Measured}}(\nu)}{L_{\text{H}}^{\text{Measured}}(\nu) - L_{\text{C}}^{\text{Measured}}(\nu)}. \quad (15)$$

The calibrated spectrum can be expressed as

$$L^{\text{Calibrated}}(\nu) = L^{\text{Measured}}(\nu) K^{-1}(\nu) - M^{\text{stray}}(\nu). \quad (16)$$

In this study, on account of the temperature of background (24.1°C), the hot temperature of the blackbody was 30.9°C and the cold temperature of the blackbody was 21.1°C. The measured (un-calibrated) spectra of the blackbody at temperatures 30.9 and 21.1°C are shown in Fig.5. The theoretical spectra are shown in Fig.6. According to expression (16), the calibrated spectrum ($L_1(\nu)$) of the measured spectrum in Fig.3 was calculated and is shown in Fig.7. The dash dot curve in Fig.7(b) represents the theoretical spectrum ($B(\nu, T)$) of the blackbody at an ambient atmosphere temperature of 8°C.

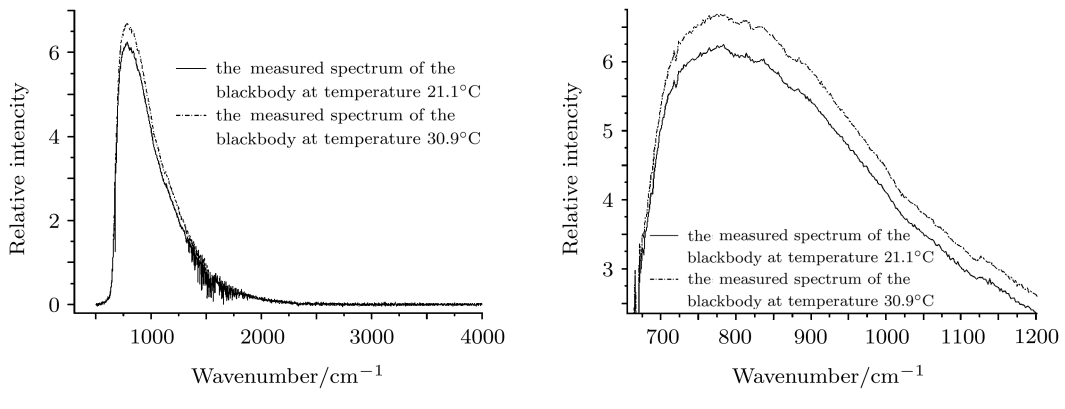


Fig.5. The measured (un-calibrated) spectra of the blackbody at temperatures 30.9 and 21.1°C.

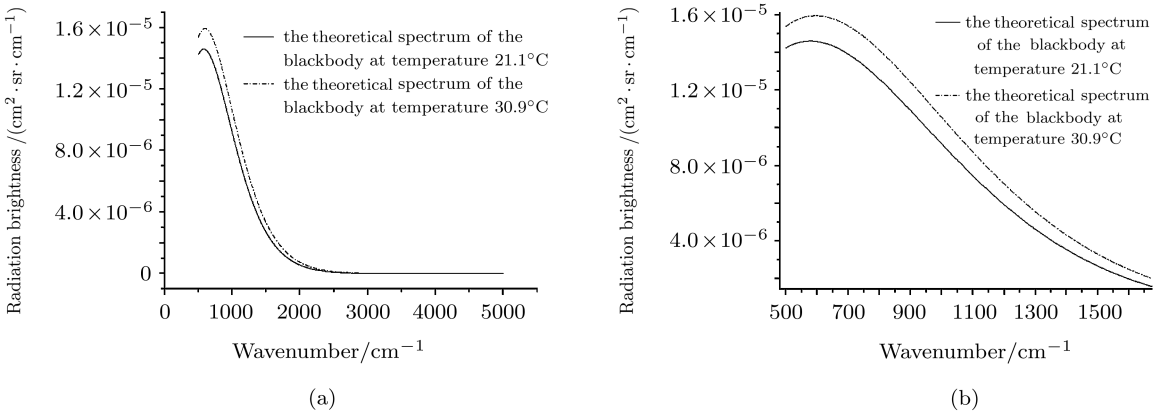


Fig.6. The theoretical spectra of the blackbody at temperatures 30.9 and 21.1°C.

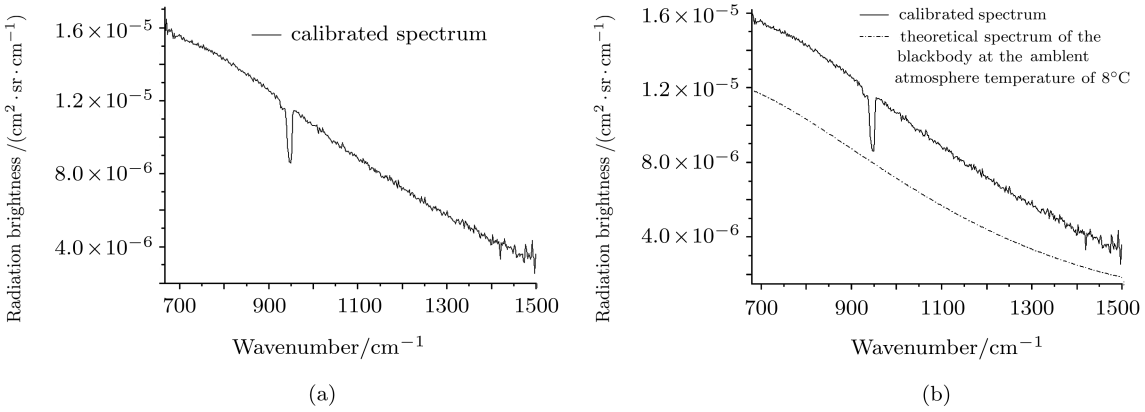


Fig.7. Calibrated spectrum ($L_1(\nu)$) of the measured spectrum in Fig.3. The dash dot curve in panel (b) represents the theoretical spectra ($B(\nu, T)$) of the blackbody at an ambient atmosphere temperature of 8°C.

4.2. Beer–Lambert law

Beer–Lambert law expresses the relationship between absorbance and concentration of an absorbing sample.[11] The absorbance of each component is independent of the absorbance of all other components. It can be written as

$$I(\nu) = I_0(\nu)\mathrm{e}^{-L\sum\limits_i \sigma_i(\nu)C_i}, \tag{17}$$

where $I(\nu)$ is the measured intensity after attenuation, $I_0(\nu)$ is the initial unattenuated reference intensity, $\sigma_i(\nu)$ is the absorption coefficient or cross section at ν of component i, C_i is the concentration of component i, L is the optical path length, and C_iL is the column density of component i along the optical path.

If a cloud with a mixture of a target component and an unknown component is expected, it is favourable to select a small spectral region for the analysis.[12]

Transmissivity $\tau(\nu)$ is expressed as

$$\tau(\nu) = \frac{I(\nu)}{I_0(\nu)} = \mathrm{e}^{-L\sum\limits_i \sigma_i(\nu)C_i}, \tag{18}$$

where $\sigma_i(\nu)$ is calculated from HITRAN Database or other infrared spectral database. In this work, the datum of the absorption coefficient of Sulfur Hexafluoride (SF_6) was taken from the HITRAN database.

4.3. HITRAN database

The HITRAN database contains spectroscopic parameters for absorption line positions and strengths for 39 molecules, including parameters for the pressure and temperature broadening effects.[13]

Temperature broadening leads to a Gaussian line shape. It is given by[14]

$$f_{\mathrm{G}}(\nu) = \frac{1}{\alpha_{\mathrm{G}}\sqrt{\pi}} \exp\left(-\frac{(\nu-\nu_0)^2}{\alpha_{\mathrm{G}}^2}\right), \tag{19}$$

and

$$\alpha_{\mathrm{G}} = \frac{\nu_0}{c}\sqrt{\frac{2kT}{m}}, \tag{20}$$

where α_{G} is the Gaussian half-with at half-height, and m is the molecular mass.

Pressure broadening leads to a Lorentzian line shape. It is expressed as[14]

$$f_{\mathrm{L}}(\nu) = \frac{\alpha_{\mathrm{L}}/\pi}{(\nu-\nu_0)^2+\alpha_{\mathrm{L}}^2}, \tag{21}$$

and

$$\alpha_{\mathrm{L}} = \left(\frac{296}{T}\right)^n (\gamma_{\mathrm{air}} \cdot (p-p_{\mathrm{s}}) + \gamma_{\mathrm{self}} \cdot p_{\mathrm{s}}), \tag{22}$$

where α_{L} is the Lorentzian half-width at half-height and is proportional to total pressure, p is the air pressure, and p_{s} is the pressure if the concerned gas is only the present gas.

The integrated line strengths are tabulated in HITRAN database at 296 K and must be corrected to the temperature of the measurement[15,16] as follows:

$$S(T) = S(296)\cdot\exp\left(-c_1\cdot E_0\cdot\left(\frac{1}{T}-\frac{1}{296}\right)\right) \cdot\left(\frac{296}{T}\right)^m \cdot \frac{1-\exp\left(-\frac{c_1\nu_0}{T}\right)}{1-\exp\left(-\frac{c_1\nu_0}{296}\right)}. \tag{23}$$

The absorption coefficient or cross section $\sigma(\nu)$ is the convolution of the integrated line strength and the line shape contributions of two kinds of broadening, i.e.

$$\sigma_0(\nu) = S(T)\otimes f_{\mathrm{L}}(\nu)\otimes f_{\mathrm{G}}(\nu). \tag{24}$$

Figure 8 shows the calculated absorption coefficient $\sigma_0(\nu)$ of sulfur hexafluoride (SF_6) from the HITRAN database at a temperature of 8°C and a pressure of 1.013×10^5Pa with a high spectral resolution.

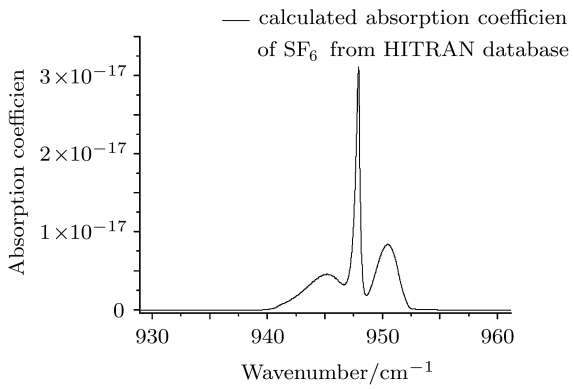


Fig.8. Calculated absorption coefficient $\sigma_0(\nu)$ of SF_6 from the HITRAN database at a temperature of 8°C and a pressure of 1.013×10^5Pa with a high spectral resolution.

In practice, it is impossible that the spectra are measured with an infinite optical path difference. One should consider not only the environmental effects (pressure and temperature) but also instrumental effects (resolution, instrumental line shape ILS(ν)). For the MR154 FTIR spectrometer, the apodization function is a boxcar apodization function. It leads to a sinc function instrumental line shape ILS(ν). $\sigma_0(\nu)$ should be convolved with ILS(ν) to produce the absorption coefficient $\sigma(\nu)$ matched with the measured spectra at a low spectral resolution,[12] and it is given as

$$\sigma(\nu) = \sigma_0(\nu)\otimes \mathrm{ILS}(\nu). \tag{25}$$

Figure 9 gives the absorption coefficient $\sigma(\nu)$ matched with the measured spectra at a low spectral resolution of $4\,\mathrm{cm}^{-1}$.[17] It was much broadened compared with $\sigma_0(\nu)$ in Fig.8.

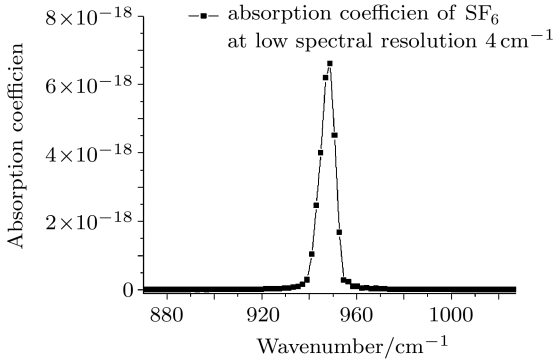


Fig.9. Absorption coefficient $\sigma(\nu)$ of SF_6 at a low spectral resolution of $4\,\mathrm{cm}^{-1}$.

4.4. Quantitative analysis

According to expressions (9) and (18), the following expression can be given:

$$\begin{aligned}&(L_1(\nu)-B(\nu,T))\\ &= (L_3(\nu)-B(\nu,T))\tau_2(\nu)\\ &= (L_3(\nu)-B(\nu,T))\cdot \mathrm{e}^{-L\sum\limits_i \sigma_i(\nu)C_i}.\end{aligned} \tag{26}$$

For active measurement, the temperature of artificial infrared light source is above 1000°C, and so the radiation entering into the spectrometer is hundreds of times more than that from the gas cloud ($B(\nu,T)$). Compared with the radiance of the artificial infrared light source, the emission of the gas cloud can be neglected.[3] Therefore, expression (26) is simplified into

$$L_1(\nu) = \tau_2(\nu)\cdot L_3(\nu) = L_3(\nu)\cdot \mathrm{e}^{-L\sum\limits_i \sigma_i(\nu)C_i}. \tag{27}$$

Expression (27) is the typical equation of Beer–Lambert law. But for the passive remote sensing, in most cases, the difference between the temperature of the gas cloud and the brightness temperature of the background is usually a few kelvins. The gas cloud emission is almost equal to the background emission. Thereby, the emission of the gas cloud cannot be ignored.

4.4.1. Cloud emission

There are several methods of obtaining the cloud emission.[17] All these methods are based on the assumption that the temperature of the gas cloud is equal to the temperature of the ambient atmosphere, under the condition of thermal equilibrium. Theses methods are separately:

To measure the emission spectrum of a black plate which is in thermal equilibrium with the ambient atmosphere. This method has an advantage that there is no need for the measured spectrum to be calibrated;

To calculate the average brightness temperature in a spectral range within which the atmosphere is opaque. The radiance of the blackbody at this temperature is taken as the emission of the gas cloud;

To measure the temperature of the atmosphere by using a thermometer. Then, the emission of the gas cloud is calculated from the Planck's function.

In the present work, the last method is used.

4.4.2. Background radiation acquirement

There are also several methods to obtain the background radiation. These methods are separately:

To measure the radiation spectrum of the background where the gas cloud is not present;[18]

To simulate the radiation of the background by using the MODTRAN and FASCOD3 if the background is the sky;[19,20]

To calculate the baseline of the brightness temperature spectrum in the spectral range of the transitions of the gas cloud to determine the radiance of the background. Figure 10 is the brightness temperature spectrum of Fig.7(a). But for some natural materials, the temperature spectrum does not have a constant baseline because the emissivity of the background is not constant with the wavelength varying in the spectral range;[17,21]

To calculate the background spectrum by using the Fourier transformation of a centre part of the measured interferogram,[3,22] which is based on the fact that from Fourier transform theory, a narrow peak in spectral space (i.e. high frequency) caused by, for example, absorption is spread out in retardation space, while a broad peak (i.e. low frequency) caused by, for example, the background becomes narrow in the retardation space;

To fit the broad background spectrum, which is a slowly varying function of frequency by using a nonlinear least squares fit algorithm.[17]

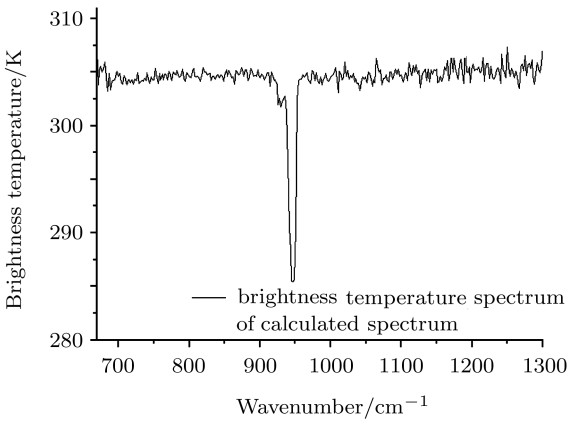


Fig.10. Brightness temperature spectrum of calibrated spectrum ($L_1(\nu)$) in Fig.7(a).

In this paper, the background spectrum was fitted with a polynomial by using the Levenberg–Marquardt method which is a kind of nonlinear least squares fitting algorithm.

4.5. Concentration retrieval algorithm

In order to simplify these equations, $L(\nu)$ and $L_0(\nu)$ are defined as

$$L(\nu) = L_1(\nu) - B(\nu, T), \tag{28}$$

and

$$L_0(\nu) = L_3(\nu) - B(\nu, T). \tag{29}$$

Figure 11 gives the spectrum of $L(\nu)$, which is the differential spectrum between the calibrated spectrum ($L_1(\nu)$) of the measured spectrum in Fig.7(a) and the theoretical spectrum ($B(\nu, T)$) of the blackbody at an ambient atmosphere temperature of 8°C in Fig.7(b).

The calculated spectrum of background is written as an n-order polynomial

$$L_0'(\nu) = a_0 + a_1\nu + a_2\nu^2 + \ldots + a_n\nu^n, \tag{30}$$

where a_i is the coefficient of the ith order term of the polynomial. In this paper, n is equal to 2. The calculated spectrum with gas cloud absorption can be expressed as

$$L'(\nu) = L'_0(\nu) \cdot \mathrm{e}^{-L\sum\limits_i \sigma_i(\nu)C_i}. \tag{31}$$

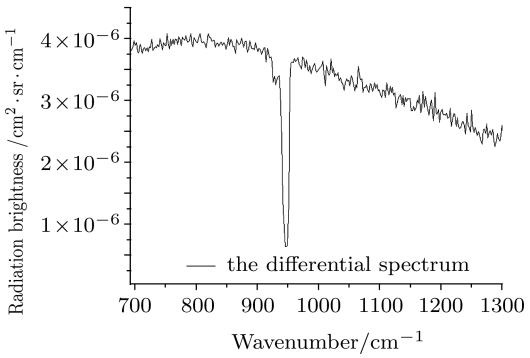


Fig.11. The differential spectrum between calibrated spectrum ($L_1(\nu)$) of the measured spectrum in Fig.7(a) and the theoretical spectrum ($B(\nu, T)$) of the blackbody at an ambient atmosphere temperature of 8°C in Fig.7(b).

All the parameters (polynomial coefficient a_i and column density C_l of the gas cloud) are retrieved by minimizing the difference between the calculated spectrum $L'(\nu)$ and the measured spectrum $L(\nu)$, i.e.

$$\chi^2 = \sum_{\nu} \left(L'(\nu) - L(\nu)\right)^2 = \text{Minmum}. \tag{32}$$

All of the above calculations were performed by using the Levenberg–Marquardt nonlinear least squares fitting algorithm in VC^{++} procedure developed by our research group. The Levenberg–Marquardt algorithm has proved to be an effective and popular way to solve nonlinear least squares fitting problems. The Levenberg–Marquardt algorithm interpolates between the Gauss–Newton algorithm and the method of gradient descent. The Levenberg–Marquardt algorithm is more robust than the Gauss–Newton algorithm, which means that in many cases it can find a solution even if it starts very far off the final minimum. On the other hand, for well-behaved functions and reasonable starting parameters, the Levenberg–Marquardt algorithm tends to be a bit slower than the Gauss–Newton algorithm. The coefficient of correlation (R) between the calibrated spectrum and the calculated spectrum is calculated. If the coefficient of correlation (R) is above the threshold and the calculated spectrum accords with the measured spectrum, the retrieved column density is acceptable. The results are shown in Fig.12. The retrieved column density of sulfur hexafluoride (SF_6) is $C_l = 133.32 \times 10^6$m. Figure 12(a) shows the fitted spectrum of background (short dot curve), the calculated spectrum (dash dot curve) and the calibrated spectrum (solid curve) of the measured spectrum. Figure 12(b) is for the spectrum of transmissivity, which is the ratio of the fitted spectrum of background to the calculated spectrum. In this experiment, the column density (C_iL) of component i only along one optical path was given. For a practical measurement, the chemical gas cloud may be a large area and non-homogeneous. A scanning FTIR system can be used for measuring the distribution of the cloud. The distribution of the cloud is shown with a false colour image. This is our further work.

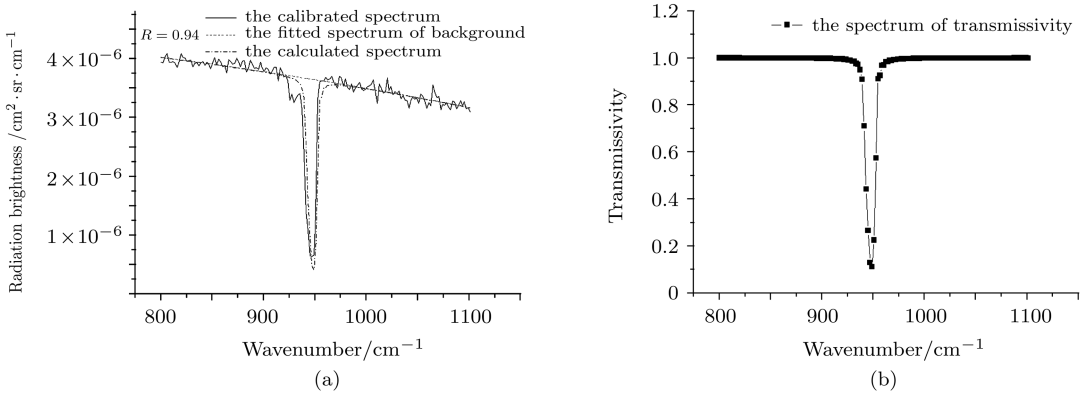


Fig.12. The fitted spectrum of background (short dot curve), the calculated spectrum (dash dot curve) and the calibrated spectrum (solid curve) of the measured spectrum (a) and the spectrum of transmissivity (b).

5. Summary and conclusions

The purpose of this paper is to present the concentration retrieval algorithm for the passive FTIR remote measurement of gas cloud in detail. A simulated experiment for sulfur hexafluoride (SF_6) is performed in laboratory. The calculated spectrum accords well with the measured spectrum. The concentration retrieval algorithm is proved by the results. The estimation of cloud temperature and the acquirement of absorption coefficient from the infrared database are the primary sources of error in concentration retrieval. This algorithm is the base of the passive remote systems (CATSI,[18] SIGIS[23]) which can be mounted on moving platforms, such as vehicles, ships, and aircrafts, etc. These systems may be used to detect the released gases and aerosols in chemical accidents, battlefield, terrorist attacks, etc.

References

[1] Beil A, Daum R, Matz G and Harig R 1998 *SPIE* **3493** 32

[2] Dennis F Flanigan 1997 *Appl. Opt.* **36** 7027

[3] Larry B Grim, Thomas C Gruber Jr and John Ditillo 1996 *Proc. SPIE* **2883** 443

[4] Pierre C Dufour, Nelson L Rowell and Alan G Steele 1998 *Appl. Opt.* **37** 5923

[5] Harig R 2004 *Appl. Opt.* **43** 4603

[6] Harig R, Rusch P, Dyer C, Jones A, Moseley R and Truscott B 2005 *SPIE* **5995** 599510

[7] Chaffin C T, Jr, Marshall T L and Chaffin N C 1999 *Field Anal. Chem. Technol.* **3(2)** 111

[8] Zeng X H, Zhao G J, Zhang L H, He X M, Hang Y, Li H J and Xu J 2005 *Acta Phys. Sin.* **54** 1000 (in Chinese)

[9] Zhu J, Liu W Q, Lu Y H, Gao M G, Zhao X S, Zhang T S and Xu L 2005 *SPIE* **5832** 83

[10] Song Y, Wang Z G, Wei K F, Zhang C H, Liu C B, Zang H and Zhou L H 2007 *Acta Phys. Sin.* **56** 1000 (in Chinese)

[11] Zhao P T, Zhang Y C, Wang L, Hu Shun X, Su J, Cao K F, Zhao Y F and Hu H L 2008 *Chin. Phys.* B **17** 1674

[12] Harig R and Matz G 2001 *Field Anal. Chem. Technol* **5**(1-2) 75

[13] Rothman L S, Jacquemart D, Barbe A, Chris Benner D, Birk M, *et al* 2005 *Quantitative Spectroscopy and Radiative Transfer* **96** 139

[14] David W T Griffith 1996 *Appl. Spec.* **50** 59

[15] Manne Kihlman 2005 *Application of Solar FTIR Spectroscopy for Quantifying Gas Emissions* Thesis for the Degree of Licentiate of Engineering, Department of Radio and Space Science, Chalmers University of Technology, Sweden

[16] Song X S, Cheng X L, Yang X D, Linghu R F and Lv B 2008 *Chin. Phys.* B **17** 1674

[17] Harig R, Matz G and Rusch P 2002 *SPIE* **4574** 83

[18] Jean-Marc Thériault, Eldon Puckrin, Huo Lavoie, Caroline S Turcotte, Francois Bouffard and Denis Dubé 2004 *SPIE* **5584** 100

[19] Dennis F Flanigan 1996 *Appl. Opt.* **35** 6090

[20] Evans W F J, Puckrin E and McMaster 2002 *SPIE* **4574** 44

[21] Dennis F Flanigan 1995 *Appl. Opt.* **34** 2636

[22] Jeffrey L Hall, Mark L Polak and Kenneth C Herr 1995 *Appl. Opt.* **34** 5406

[23] Harig R, Matz G, Rusch P, Gerhard H H, Gerhard J H and Schlabs V 2005 *SPIE* **5995** 59950J